THE GEOLOGICAL SOCIETY OF AMERICA®

Low sinuosity meandering rivers before vascular plants: Cambrian Tapeats Formation, Arizona, USA

Paul M. Myrow[1,†], Robert R. Gaines[2,†], and Michael P. Lamb[3]
[1]*Department of Geology, Colorado College, Colorado Springs, Colorado 80903, USA*
[2]*Geology Department, Pomona College, Claremont, California 91711, USA*
[3]*Division of Geological and Planetary Sciences, California Institute of Technology, Pasadena, California 91125, USA*

ABSTRACT

A longstanding view is that rivers in pre-Silurian landscapes, prior to the colonization of continents by land plants, were braided and that meandering rivers—characterized by lateral migration to the point of bend cutoff—were rare. Evidence for this view includes river deposits dominated by amalgamated sandstone and a lack of muddy floodplain deposits that typify modern meandering river systems. Here, we present detailed analysis of pre-Silurian fluvial deposits from the lower Cambrian Tapeats Formation, Arizona, USA, with low levels of mudstone, but that nonetheless contain evidence for low sinuosity meandering rivers in a sandy floodplain. Channelized granule to pebble conglomerate, pebbly sandstone, and medium-grained sandstone bodies up to 1.2 m thick contain point-bar lateral accretion surfaces, indicating lateral migration of meandering rivers. Low-angle outer-bend channel margins (~10°) may reflect small proportions of floodplain mud at the channel cutbank. Stratal geometries indicate multiple episodes of channel abandonment, many of which occurred when channels migrated only 1–2 channel widths with little or no channel-bed aggradation, suggesting a chute cutoff mechanism. Three intervals record abandonment at times of channel setup (superelevation of bankfull water level above the floodplain) when the channel floor increased in elevation by only 25%–75% bankfull depth, well below values typical of avulsion (~100%). All of this indicates unstable channels and early abandonment compared to modern meandering rivers. Unlike vegetated meandering rivers, for which bends often grow to the point of neck cutoff, bend growth in pre-Silurian rivers was limited by channel abandonment through the rapid development of chutes across the easily erodible, vegetation-free, and predominantly sandy floodplains.

INTRODUCTION

Meandering rivers of various scales are a primary control on terrestrial geomorphology as they sweep laterally across muddy floodplains through erosion on their outer banks and point-bar deposition on their inner bends. The evolution of land plants had a profound effect on fluvial processes, and the dynamics of earth surface processes in general, through the sequestration of mud on floodplains by baffling flow and promoting organic-induced flocculation of mud, which enhances settling and mud retention. The reigning paradigm has been that before the proliferation of land plants in the Silurian, wide and shallow (sheet-braided) rivers dominated (Cotter, 1978) and that meandering rivers would have had unstable banks and thus been rare and short lived (Davies and Gibling, 2010; Santos and Owen, 2016). Recent work on modern meandering rivers in unvegetated to poorly vegetated regions (Matsubara et al., 2015; Ielpi, 2017, 2019; Hasson et al., 2023) and physical experiments support the idea that meandering rivers can form in the absence of land plants, as indicated by martian deposits (DiBiase et al., 2013; Kite et al., 2015; Hayden et al., 2021). Studies of pre-Silurian rocks, primarily Precambrian (Paleoproterozoic to Mesoproterozoic) strata (Long, 1978, 2011; Sarkar et al., 2012; Ielpi and Ghinassi, 2015; Ielpi and Rainbird, 2016; Went, 2017; Ielpi et al., 2018), indicate that ancient meandering river deposits existed (e.g., Ielpi et al., 2017; Ganti et al., 2019; Valenza et al., 2023), although they are relatively less abundant than braided stream deposits. Braided streams form amalgamated sand and gravel bodies in the absence of thick mud layers, which on vegetated floodplains provide strength that slows cutbank erosion, channel widening, and ultimately meander bend growth. Bank strengths in pre-Silurian, unvegetated floodplains could have been provided by early cementation, or by mud cohesion since only a small amount of mud (~10%) is needed to add significant strength to a granular deposit. Regardless of the mechanism, sand- and gravel-dominated meandering rivers on Earth prior to vegetated terrestrial landscapes would have had potentially significantly different dynamics.

We present a detailed sedimentological analysis of strata of the Tapeats Formation (Cambrian Series 2) of central Arizona, USA, with well-developed, channel-form fluvial facies that provide a glimpse into the depositional dynamics of small single-thread Pre-Silurian meandering rivers. These dynamics include aspects of the nature and frequency of channel abandonment, and the resulting stratigraphic record of such behaviors.

STUDY AREA

The lower Cambrian Tapeats Formation is widely exposed across Arizona, including its type area in the Grand Canyon (Rose, 2006; Karlstrom et al., 2020) where it sits on the great unconformity. At most sections, the Tapeats was deposited unconformably on Archean and Proterozoic basement rocks during the Sauk Transgression (Karlstrom et al., 2018). The formation contains a variety of fluvial and marine facies (Hereford, 1977; Rose, 2006; Fedo and Cooper, 1990; Dehler et al., 2024), with a transition from fluvial facies to the southeast and more marine facies to the northwest (Rose, 2006; Hereford, 1977). The Tapeats was deposited in the last 2 m.y. of Series 2 (Stage 4) of the Cambrian: ca. 508–507 Ma (Karlstrom et al., 2018, 2020).

In the Payson area, the Tapeats Formation rests nonconformably on Paleoproterozoic basement

Paul M. Myrow https://orcid.org/0000-0003-3253-3699
[†]Paul M. Myrow, pmyrow@coloradocollege.edu; Robert R. Gaines, Robert.Gaines@pomona.edu

GSA Bulletin; January/February 2026; v. 138; no. 1/2; p. 809–822; https://doi.org/10.1130/B38336.1.
Published online 9 September 2025

and is disconformably overlain by the Devonian Martin Formation, with an unknown thickness of Tapeats removed by erosion at the sub-Devonian unconformity (Hereford, 1977). Paleomagnetic data from Elston and Bressler (1977), regional facies relationships (Hereford, 1977), and detrital zircon age spectra from across the region (Karlstrom et al., 2018, 2020; Matthews et al., 2018) support a Cambrian age.

Hereford (1977) identified multiple facies associations in the Tapeats, ranging from a marine shoreline setting in the northwest (Grand Canyon area) to fluvial facies in the southeast. The Payson area contains the easternmost (landward) exposures of the Tapeats Formation (Hereford, 1977), and it lies within a fluvial facies belt that is ~45–75 km southeast of an inferred marine–nonmarine transition zone, although Hereford (1977) did interpret a few thin intervals of possible intermittent tidal influence ~25–55 km inland from that facies transition. Given that Hereford's work was done prior to the development of many shallow marine facies models (e.g., for storm- and wave-influenced shorelines and shelves), it is unclear if these thin channel deposits in fact represent tidal influence. If the Tapeats in the Payson area is in fact fully lower Cambrian, then other reconstructions (Dehler et al., 2024, their fig. 4; Rose, 2006, his fig. 2) would place the lower Cambrian shoreline as far west as the central Grand Canyon region at the time of deposition.

METHODS

We examined outcrops of the Tapeats Formation in the vicinity of the town of Payson, Arizona, over an area of ~120 km^2 (Fig. 1), ~200 km south-southeast of the Grand Canyon, including roadcuts just north of town along Route 87, and natural outcrops in hills both farther north and east of town. Sections were logged in cm-scale detail and covered intervals were measured using a Jacob staff and Brunton compass. Mode, maximum, and minimum grain size were assessed for each bed using a grain size card and hand lens. The sizes of pebble- to boulder-sized clasts were measured with the aid of a tape measure. A grid survey clast size count was made of 100 clasts from pebble to cobble conglomerate at Wildcat Springs E (East Locality) (Figs. 1 and 2B). Paleocurrents were assessed by measurement of dip direction orientations of dune-scale cross-bedding foresets; ripple-scale cross-bedding is generally absent because the grain sizes are generally outside the stability field of ripples (too coarse). Some locations have few data points, but these are consistent with the majority of the paleocurrent data, which are in turn consistent with the much larger suite of paleocurrents provided by Hereford (1977).

Photomosaics were assembled in Adobe Photoshop and hand annotated in the field with direct observations of sedimentary structures, relationships among beds, and facies interpretations. Annotations were then digitized onto the photomosaics using Adobe Illustrator. Clay mineralogy was assessed using <2 μm separates, isolated by centrifugation, air-dried on ceramic tiles, and analyzed using a Rigaku Ultima IV X-Ray diffractometer at Pomona College, Claremont, California, USA. The presence of kaolinite was verified by peak collapse after heating to 550 °C.

RESULTS

Strata East of Payson, Arizona

Based on regional mapping of the formation, the eastern part of the study area represents the easternmost exposures of the Tapeats Formation. Outcrops in the area have basal units of cobble to boulder conglomerate that rest inside bedrock incised valleys that are several meters deep and include clasts up to 28 × 15 × 18 cm in size (Figs. 2 and 3). Cobble conglomerate beds, up to 2.8 m thick, are strongly imbricated and have clast-supported textures (Figs. 2 and 3A–3D). One 66-cm-thick bed at Diamond Point has a matrix-supported texture (Fig. 2C). The strata above the basal cobble to boulder conglomerate beds at these locations are dominated by poorly sorted granule to cobble conglomerate and very coarse sandstone. The internal structures of these deposits range from massive to crudely parallel laminated to trough cross-stratified, the latter ranging from ~10 cm to 100 cm thick (Figs. 2 and 3).

The grid survey of pebble to cobble clasts at Wildcat Springs East (Figs. 1 and 2B) yielded sizes from 2 mm to 150 mm in diameter and an average grain size of ~2.7 cm. Paleocurrent data for the locations north and east of Payson (Figs. 4C–4F) indicate flow dominantly to the south and west. The vector mean of all the data is 213°. Paleocurrent data collected across Arizona by Hereford (1977, his fig. 1) range from south to north but are primarily oriented WSW, which is somewhat oblique to the NW-SE–oriented outcrop belt.

Strata of Payson, Arizona

The following are facies descriptions for an outcrop of the Tapeats Formation located immediately north of the town of Payson, Arizona (Figs. 1 and 4), where the Tapeats is well exposed in a roadcut exposure on Route 87 (labeled 87S on Fig. 1). Here, the formation is dominated by laterally discontinuous beds of granule to pebble conglomerate, pebbly sandstone, and medium sandstone that are centimeters to >1 m thick (Fig. 5). The sandstone and conglomeratic sandstone beds have channel-form geometries and cross-bed sets a few tens of centimeters to >1 m thick, and these beds are the focus of this study.

These poorly sorted coarse deposits are interbedded with dark red shale beds up to 28 cm thick (Figs. 6 and 7D–7F). The shale beds are rich in Fe-oxides and include minor amounts of angular to subangular silt and fine sand grains in mm-scale laminae. At site 87S, shale makes up ~7.5%–13% of the outcrop by thickness (Fig. 6), which contrasts strongly with other well-documented exposures of the Tapeats to the northwest that lack shale entirely (Karlstrom et al., 2020). The shale makes up discontinuous beds that are commonly truncated from above by channelized sandstone and conglomerate units (Figs. 5–7). Intraclasts of the shale are common within conglomerate and sandstone beds. X-Ray diffraction of clay separates indicates that the clay fraction of the shale is dominated by kaolinite, verified by peak collapse upon heating to 550 °C. The clay lacks characteristic marine clay minerals such as glauconite and berthierine. In the study area, kaolinite is common in paleoweathering profiles developed into the underlying basement (Colwyn et al., 2019). At one study location, a thick paleo-

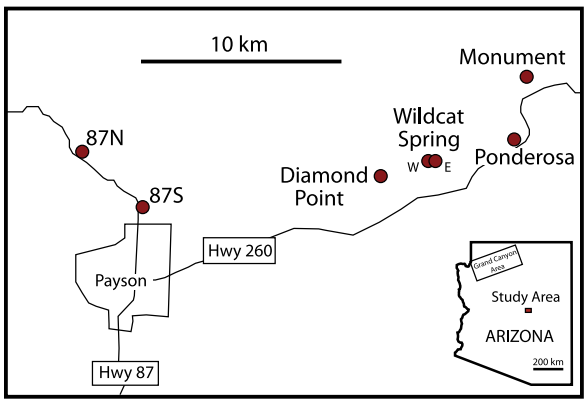

Figure 1. Location map showing location of field sites in central Arizona, USA. Proximal locations with coarse conglomeratic units to the east, and sites with sinuous fluvial channel deposits to the west.

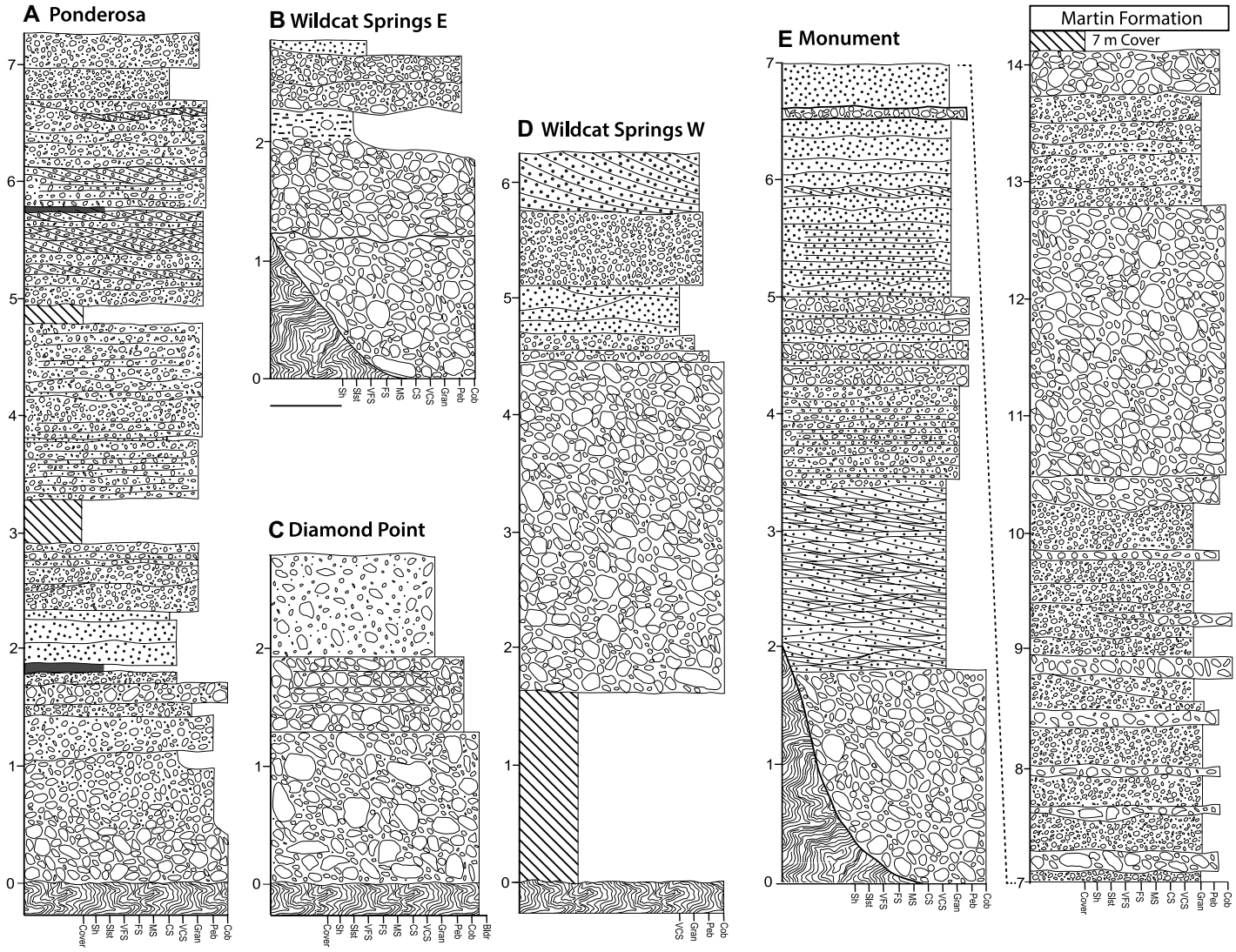

Figure 2. Measured sections for lower parts of the Tapeats Formation at locations east of the town of Payson, Arizona. Basal cobble to boulder conglomerate units rest within bedrock incised channels with relief up to ~2 m at Monument and Wildcat Springs East localities (B, E). The Monument section (E) preserves a near complete section (with 7 m cover at top). Scales are in meters. Sh—shale; Slst—siltstone; VFS—very fine sandstone; FS—fine sandstone; MS—medium sandstone; CS—coarse sandstone; VCS—very coarse sandstone; Gran—granule conglomerate; Peb—pebble conglomerate; Cob—cobble conglomerate.

sol profile rests below the Tapeats and is cut by a basal channel of the Tapeats, which comprises a lag that includes soil clasts.

Channel-Form Cross-Bed Sets

Detailed analysis was made of three well-developed, channel-form beds (Figs. 5 and 6) at site 87S with cross-bed sets that reach up to the full thickness of the channel form, in cases up to ~1.1 m thick, and have dip angles well less than the angle of repose. Two closely spaced sections were measured at the outcrop (Fig. 6). Photomosaics of the three beds were created and the images were distorted in order to "unfold" the bedding at the south end of the outcrop that makes up the limb of a gentle fold (Figs. 8–10). Each bed is described in detail below.

The lowermost bed, Bed 1, is present in section 2 (3.97–4.58 m) but does not extend across to measured section 1 (Fig. 8). The bed, which consists of medium sandstone, pinches out over a lateral distance of 16 m. The bed overlies another channel-form deposit with a lower cross-bedded medium sandstone division and an upper division of massive pebble conglomerate. The base of Bed 1 was erosional, as shown by a truncation of an 18-cm-thick bed to the south (Fig. 8). The southern end of the bed is not fully preserved, in part because the top of the bed is truncated in this area by an erosional surface along the base of an overlying channel-fill bed (Fig. 7B). However, at both ends of Bed 1, the base of the bed rises toward the upper surface, and thus, the bed is lenticular. The foresets of the cross-bedding have a maximum dip of ~20° and they downlap onto the lower surface across much of the outcrop (for ~9 m; Figs. 7A, 7B, and 8), but then flatten out to the north, recording a shift to both lateral migration and vertical aggradation of the channel floor. Near the center of the exposure, there are several foresets that show nearly complete rollover to horizontality. The top of Bed 1 is relatively flat at the level of the rollover.

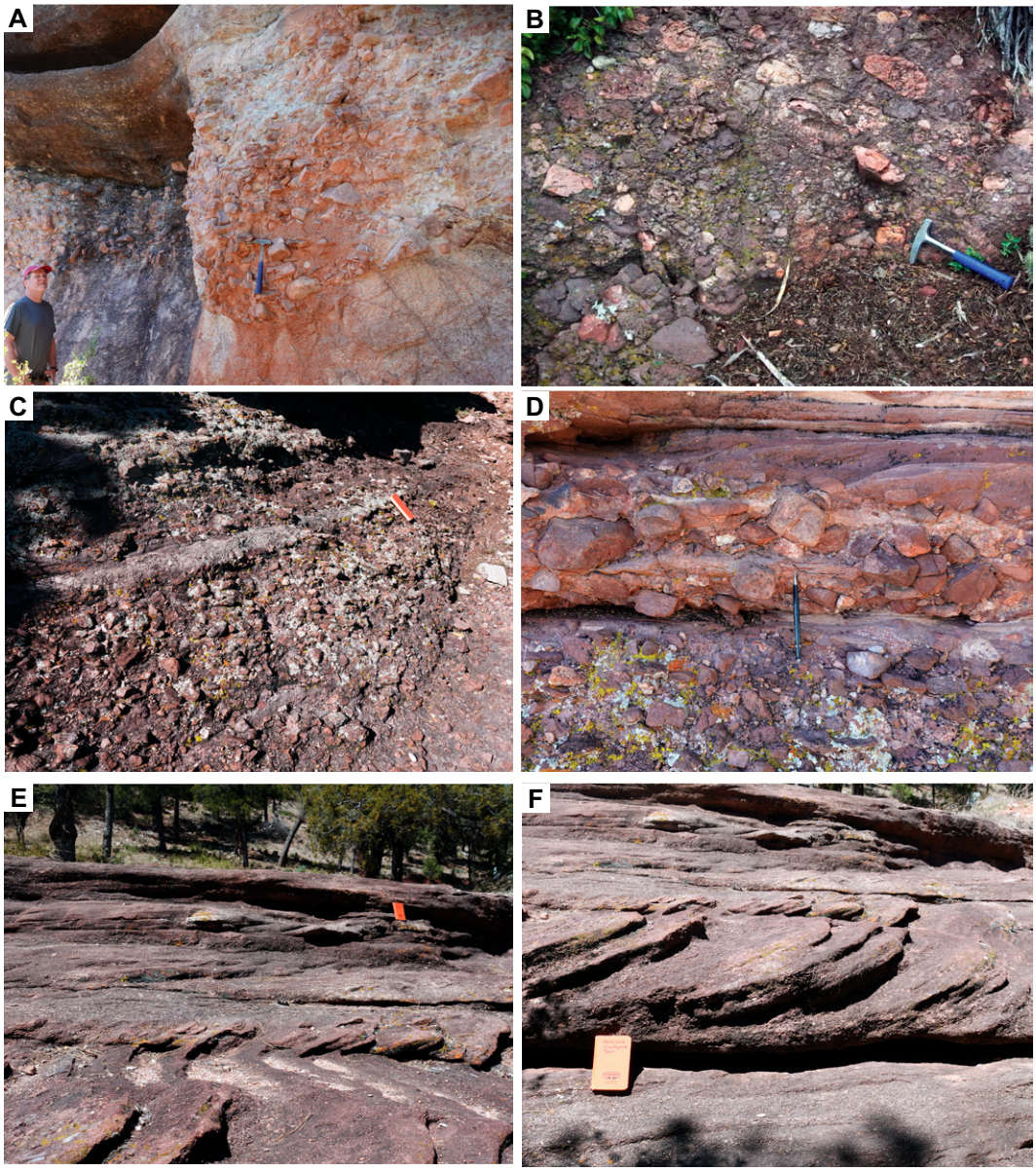

Figure 3. Proximal deposits. (A) Cobble conglomerate incised into bedrock with ~2 m of relief at Monument location. (B–D) Conglomeratic facies in proximal sections. (B) Note well developed imbrication indicating flow from right to left. (E, F) Trough cross-bedding at the Ellison Creek section. Hammer (A, B) is 30 cm long. Notebook (C, E, F) is 15 cm tall. Pencil (D) is 14 cm long.

The middle bed, Bed 2 (Figs. 7B and 9), is a channel-form deposit of granule to pebble conglomerate in section 1 (5.64–6.72 m) with a steep margin along the south end of the bed that truncates relatively flat-lying strata. The stratigraphically highest underlying truncated layer is a 20-cm-thick (maximum) shale bed. The foresets of the lateral accretion beds parallel the margin of the paleochannel and extend across up to ~20 m of the outcrop before they flatten out at the end of the exposure. Their maximum dips are ~16° and are gently to strongly tangential at the base. In most cases, erosion along the base of the overlying granule conglomerate bed resulted in truncation of the uppermost part of the foresets, but in several places a nearly complete rollover of the top of the foreset is preserved, including a cross-bed set in an exposure across the road from the main outcrop on Route 87 (Fig. 5) at a similar stratigraphic level.

There are two layers of shale that partially drape the foresets. The first (resting on pause plane 1; Figs. 9 and 7C) is up to 25 cm thick. It onlaps ~80% of the width and height of the underlying foreset and extends as a thin layer (<15 cm) for more than 6.5 m along the base of the bed to the north, eventually draping a concave-up basal erosion surface that defines the northern margin of the channel form. Subsequent overlying coarse-grained foresets downlap onto the thin, flat extension of this shale bed. A second, thin (up to 15 cm) shale bed (resting on pause plane 2, Fig. 9) onlaps a much smaller foreset and rapidly flattens out. The position of this second shale layer is significantly (70 cm) stratigraphically higher than the base of the overall channel-form bed, and it rests on a much smaller and less steep foreset that records both lateral migration and a small amount of channel-floor deposition.

Bed 3 is 66–90 cm thick in section 1 (7.45–8.33 m) and 1.13 m thick in section 2 (6.97–8.1 m; Fig. 10). It consists entirely of poorly sorted pebble conglomerate. The base of the cross-bed set rises to the south but the margin of channel-form (cf. Bed 2) presumably lies beyond the southern limit of outcrop exposure. The bed extends for up to ~20 m, but the well-defined cross-beds are present for ~16 m at the southern end of the outcrop; at the northern end, the bedding flattens out into horizontality. The

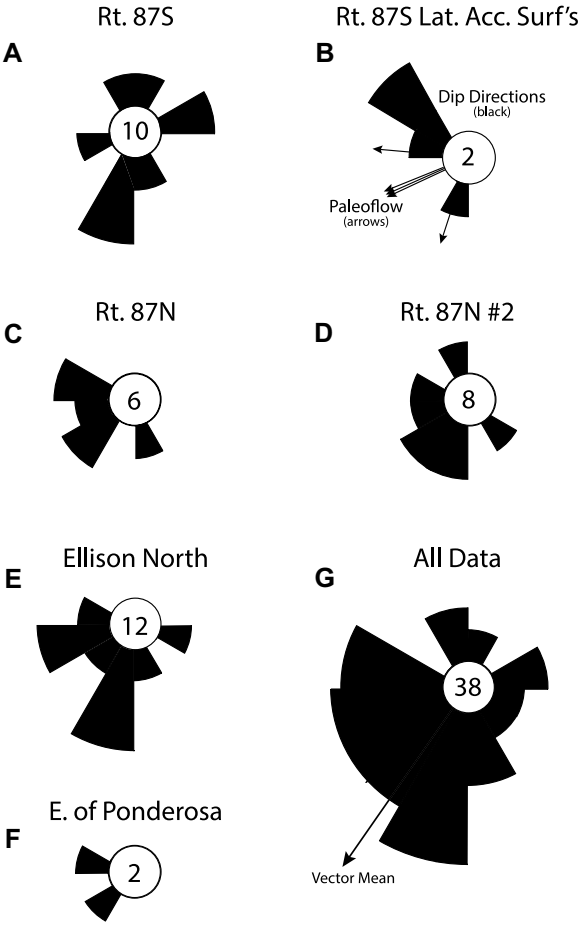

Figure 4. Rose diagrams showing paleocurrent directions measured from dune-scale trough and tabular cross-bedding. See Figure 1 for locations. (B) shows the dip directions of lateral accretion surfaces (Lat. Acc. Surf's) from the Route (Rt.) 87S locality and the interpreted paleoflow directions (arrows).

maximum dip of foresets in the bed is ~15°. The thickness of the cross-bed set thins to the north, with the bases of the foresets rising in that direction in two distinct episodes, thus defining three intervals of foreset migration separated by reorganization of stratal geometries (Fig. 10). In each of the three intervals, the foresets are initially steep and show downlap into troughs, but subsequent ones do not downlap onto a surface but instead extend as relatively evenly thick beds parallel to the relatively flat trough of the channel form, indicating both lateral migration and channel-floor deposition. The youngest foreset of the bed is nearly flat lying and directly overlain by a lens of shale that is up to 17 cm thick (Fig. 10).

INTERPRETATION

The sedimentological evidence indicates that the three beds described above record fluvial channels that migrated laterally over time. This is supported by the (1) concave-up erosional surfaces that truncate relatively flat-lying strata (e.g., Bed 2; Fig. 9), (2) lenticular geometries, and (3) cross-bedding that parallels the orientation of the preserved channel margins (e.g., Bed 2; Fig. 9). Multiple characteristics of the cross-bedding indicate that it was not produced by dunes, but instead represent lateral accretion surfaces produced by migration of a margin-attached bar, i.e., a point bar, of a meandering river. These include (1) low dips (<20°); (2) local presence of rollovers of the foresets that indicate nearly full preservation of a bar; (3) uniformity of dips of these surfaces in all three beds in a single direction across distances that are large (up to >20 m) relative to the bar heights (~1 m); and (4) dip directions (NW) that are perpendicular to general regional transport directions (SW). By contrast, braided stream deposits tend to record multiple dip directions within a single story. Braid plain deposits also typically have mid-channel bar deposits with abundant convex-up clinoforms with rollovers, commonly on both sides of the bars (Bridge, 2003), which are features that are absent in the Tapeats. Even in ancient meandering fluvial facies, mid-bar deposits are spatially limited and show highly variable accretion directions. The great extent of the lateral accretion surfaces in the Tapeats, and generally dips, are typical of point bars relative to downstream-migrating mid-bar strata, which have foresets that reach the angle-of repose.

Most of the Route 87S outcrop consists of channel-fill deposits, and several beds besides Beds 1–3 described above have large-scale cross-bedding that may also record point-bar migration. Strike orientations, adjusted for bed dip, for large-scale cross-beds that are interpreted as lateral accretion surfaces (including Beds 1–3) are 188°, 288°, 335°, 338°, and 336° (Fig. 4B). The inferred paleocurrents range from W to SSW (198°–275°), which is consistent with

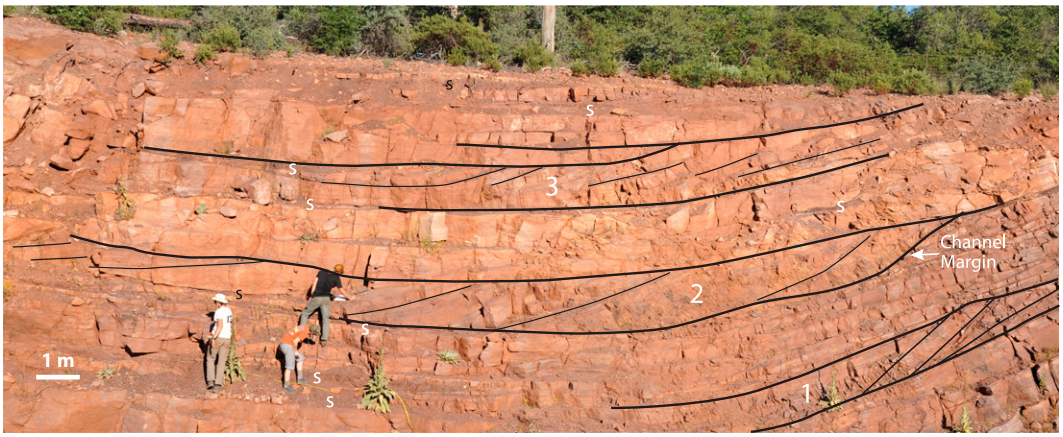

Figure 5. Exposure on Route 87 (site 87S). The three beds with well-developed lateral accretion surfaces are numbered and their geometries and internal structures are highlighted (details of each are shown in Figs. 8–10). S—shale.

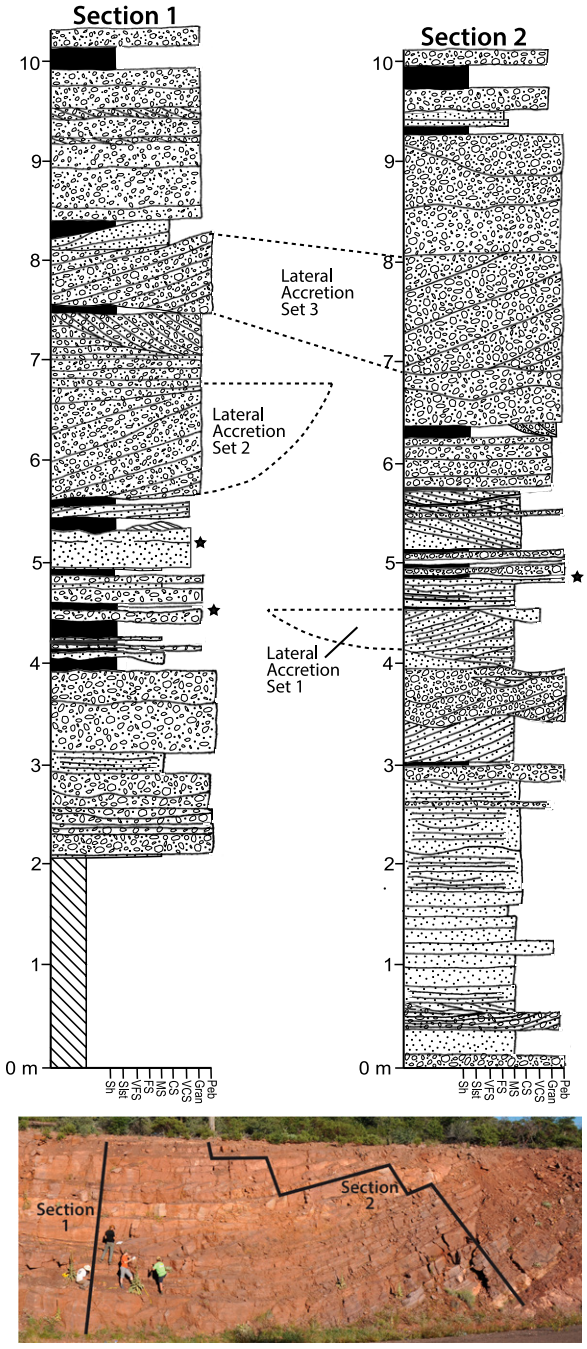

Figure 6. Closely spaced stratigraphic sections in exposure on Route 87 (site 87S). Vertical scale is in meters. Photo at base shows transect for each section. The section is gently folded on right. Sh—shale; Slst—siltstone; VFS—very fine sandstone; FS—fine sandstone; MS—medium sandstone; CS—coarse sandstone; VCS—very coarse sandstone; Gran—granule conglomerate; Peb—pebble conglomerate.

the full dataset of paleocurrents for the region (Fig. 4G). Thinner cross-bed sets (several tens of centimeters thick or less) are considered the deposits of dunes that occupied shallow channels, which either lacked migrating point bars or had migrating point bars that due to local curvature of the channels migrated in a direction that was not close to parallel to strike of the outcrop face. For the latter, the lateral accretion surfaces would be difficult to identify in cliff exposures in the plane of the outcrop as they would have low apparent dips. Dune-scale cross-bedding not identified as lateral accretion surfaces has a strong paleoflow mode to the S–SW generally perpendicular to the dip of the lateral accretion surfaces (Figs. 4A and 4B). These readings are more scattered at this outcrop with meandering river facies (Route 87S) than those at other outcrops (Figs. 4C–4F) that lack evidence of meandering river facies.

The three beds of the Tapeats described in detail above display evidence of abandonment, reoccupation, and adjustments of channel geometries. Owing to the evidence for lateral accretion of bank-attached bars in single channels, and the lack of evidence for mid-channel bars, we interpret the Tapeats channels at Route 87S to be deposits from meandering rivers. That is, single thread rivers with substantial components of bar migration that are orthogonal to river flow owing to bend expansion, which experienced cycles of bend growth and abandonment. Here we use the tripart classification of river planform by Leopold and Wolman (1957) between braided, meandering, and straight planform morphologies.

Meandering rivers migrate by lateral and downstream migration of channels and evolve toward increasing radius of curvature (Hooke, 2023). In such a system, channel abandonment results from a variety of mechanisms, including neck cutoffs, chute cutoffs, and avulsions. Neck cutoffs result from prolonged migration and increased sinuosity of channels. Chute cutoffs result from upstream, headward erosion of a chute during overbank flows. Avulsions occurring in rivers with fixed channels typically have higher aggradation rates in the channel and levee system than in the adjacent flood plain (Mohrig et al., 2000), which produces a setup (superelevation of the bankfull water level above the low point of the floodplain). The gravitational instability caused by the setup leads to avulsion when triggered by flooding over the banks and breaching of the levees. Chute cutoffs would result in abandonment of one river bend, whereas avulsions would generally result in abandonment of multiple bends.

We analyze the geometric aspects of the channel fills in each bed to interpret the mechanisms of abandonment. Neck cutoffs would be reasonably deduced if the migration distance of a channel was many times the channel width. Distinguishing between chute cutoffs and abandonment in ancient rocks mostly from cliff exposures (2-D paleo-Earth-surface exposures do not exist) is more difficult, as one could not detect if one meander bend or multiple bends were abandoned. However, it is possible to estimate the amount of setup of a channel from detailed geometric analysis of cliff exposures.

Paleohydraulic Analysis

Paleohydraulic analyses allow for the reconstruction of fluvial systems, including the nature of sediment transport, depositing flows, and the morphodynamics of channel systems (e.g., Hayden et al., 2021). Stratal geometries of the Tapeats fluvial deposits allow us to reconstruct a Cambrian fluvial system that formed in the absence of land plants and discern the behavior of channels in such systems.

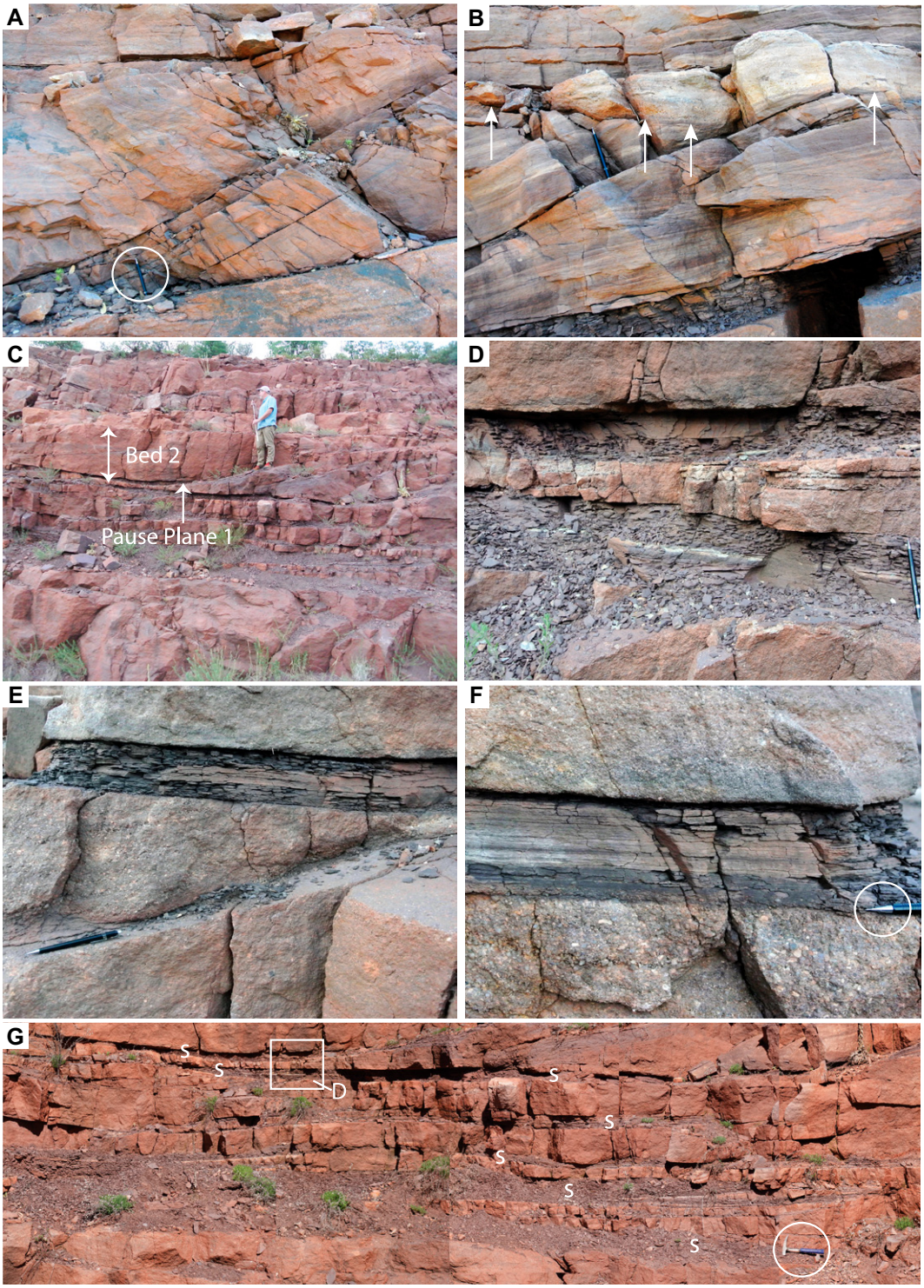

Figure 7. Photographs of facies and beds at Route 87 locality (site 87S). (A, B) Lateral accretion bedding in Bed 2 (Fig. 8) showing downlap of concave-up surfaces. Part B shows underlying shale bed that is cut out laterally (to the north) and truncation by overlying scour surface (white arrows). (C) Lateral accretion bedding in Bed 2; person standing on pause plane 1 (Fig. 9). Note abundant shale above thick conglomerate bed at base. (D) Shale-rich interval. Note location of photograph in part G. Pencil (A, B, D–F) is 14 cm long; tip is 2 cm long (F). Hammer (G) is 30 cm long. S—shale.

Migration Distance

Meandering channel wavelengths are ~12 channel widths (Hayden et al., 2021, their fig. 3A), and if neck cutoffs occur when a channel migrates approximately a full wavelength, ancient channel deposits should record migration distances of 12 channel widths, although a more conservative estimate of migration distance before cutoff is 5–7 channel widths (Howard and Knutson, 1984). Based on our photomosaics and detailed mapping of the features in each of the three channel-form beds (Figs. 8–10), we measured the approximate widths and heights of the preserved point bars (Table 1). Using this data, we estimate channel widths in two ways, with width/depth ratios. Greenberg et al. (2021) show that modern channel widths are 2.34 ± 0.13 times the measured point-bar widths. The bankfull width-to-depth ratios of modern meandering rivers are generally 10:1–20:1 (Parker et al., 2007). Using the width of the preserved point bars and heights of lateral accretion sets with rollovers (or near rollovers), we made two estimates of channel widths for each phase of devel-

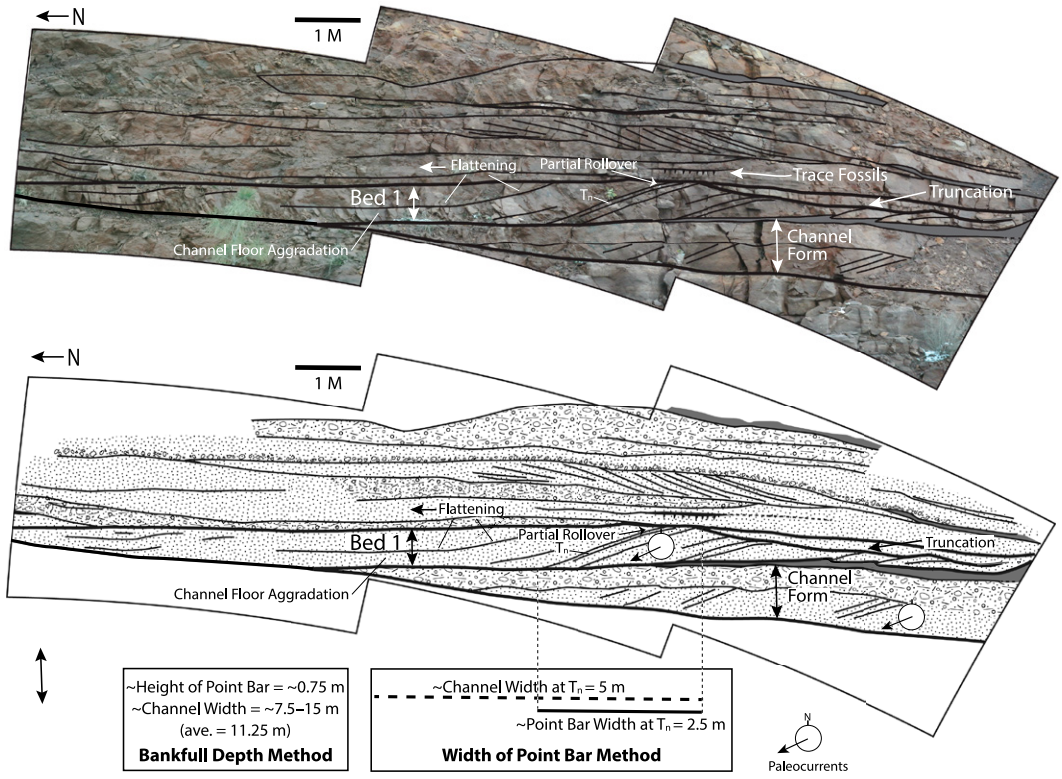

Figure 8. Lateral accretion Bed 1 photograph and sketch showing underlying channel form, lateral accretion surfaces, and truncation by small channel form at top on right. Note flattening of lamination to north. Paleocurrents are plotted as rose diagram; note that inferred paleocurrents for lateral accretion surfaces are perpendicular to the dip direction.

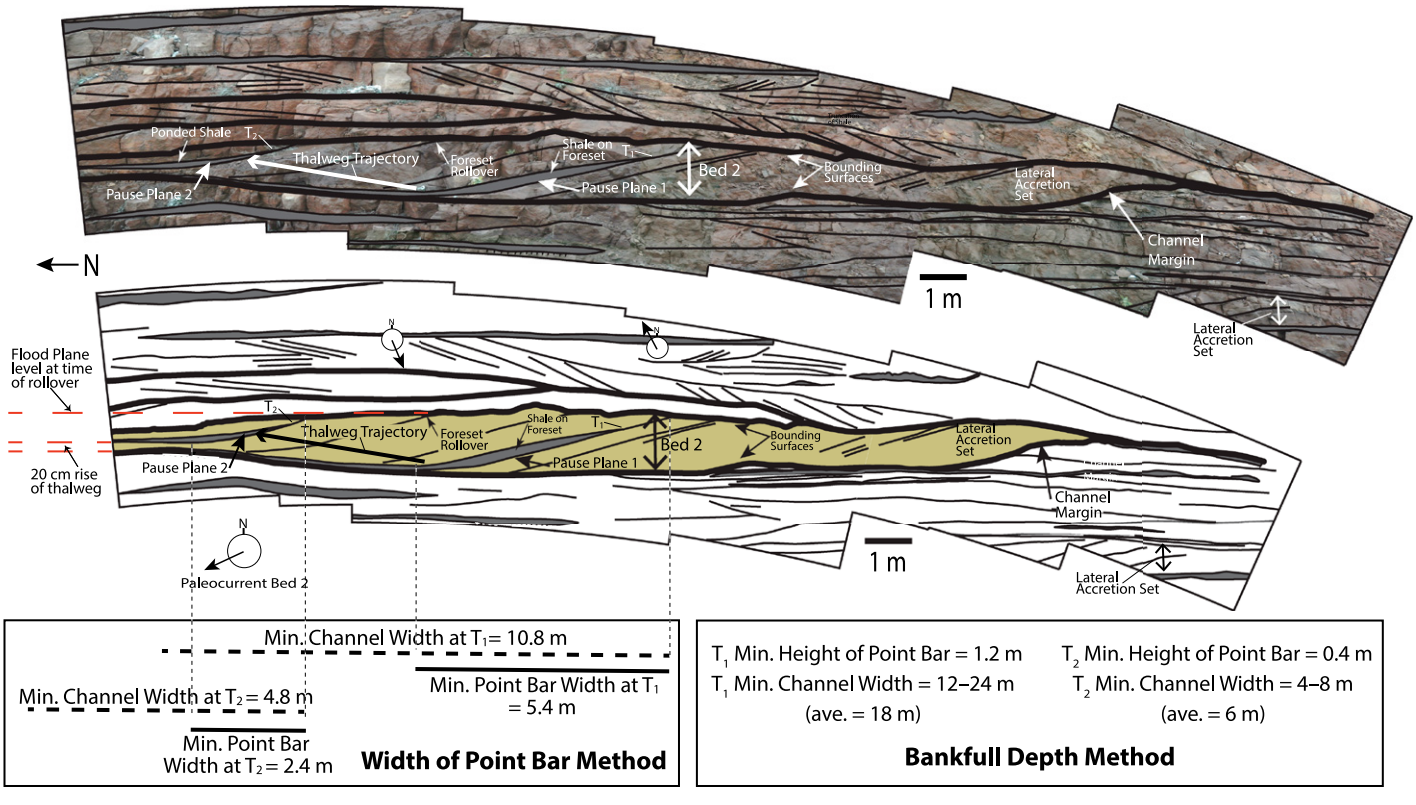

Figure 9. Lateral accretion Bed 2 photograph and sketch. Note two pause planes (1 and 2), well-preserved channel margin, and well-defined channel floor trajectory. Estimates of channel width, using two methods, are shown at base. Paleocurrents are plotted as rose diagram; note that inferred paleocurrents for lateral accretion surfaces are perpendicular to the dip direction.

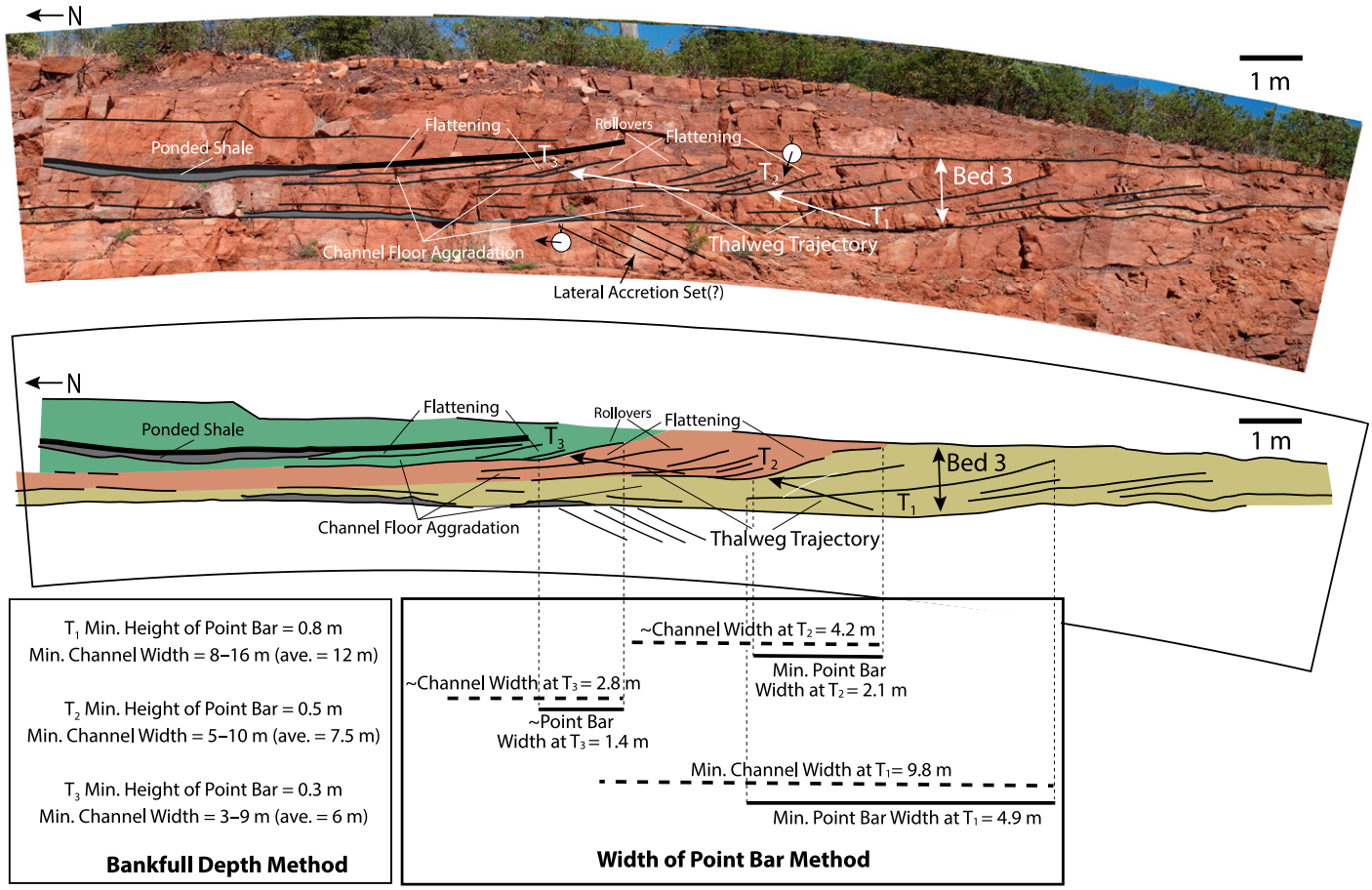

Figure 10. Lateral accretion Bed 2 photograph and sketch. The three phases of channel migration and channel-floor aggradation are shown in the three colors. Estimates of channel width, using two methods, are shown at base. Paleocurrents are plotted as rose diagram; note that inferred paleocurrents for lateral accretion surfaces are perpendicular to the dip direction.

TABLE 1. ESTIMATED CHANNEL WIDTHS

		Width of bar method		Height of bar method		
		Width of bar (m)	Estimated channel width (m)	Height of bar (m)	Estimated channel width (m)	Measured bar migration distance (m)
Bed 1		2.5	5.75	0.75	7.5–15	9
Bed 2	T_1	5.4	12.4	1.2	12–24	~20
	T_2	2.4	5.5	0.4	4–8	—
Bed 3	T_1	4.9	11.3	0.8	8–16	~8.5
	T_2	2.1	4.8	0.5	5–10	5.5
	T_3	1.4	3.2	0.3	3–9	~3
Average		3.1	7.2	0.7	10.0	

opment of the three investigated beds (Beds 1–3; Table 1). The average estimated channel width using the width of the point bars approach is 7.2 m. Using the measured thicknesses of the point bars and the median value of the estimated range of the channel widths (15 × bar height), the average estimated channel width is 10.0 m. Measured distances of lateral accretion for the Tapeats channels range from 3 m to 20 m (Table 1), which indicates that the channels generally migrated a distance of less than two (average ~1) channel widths (Table 2), as estimated from both point-bar widths and heights, before an abandonment event took place. Thus, the Tapeats channels migrated distances that were far less than modern meanders that migrate to the point of neck cutoff (a distance of at least 5–7 channel widths), indicating that the channels were not abandoned by neck cutoffs.

Although direct measurement of sinuosity of the Tapeats channels is not possible, given the lack of extensive bedding plane exposures, the short migration distances indicate very low levels of sinuosity. We use the term "low sinuosity" herein in a qualitative manner, not in a quantitative sense (i.e., lower than a cutoff of 1.4 between low and high sinuosity, as suggested by Galeazzi et al., 2021). Given our inability to measure the sinuosity values directly due to the lack of planform outcrop exposure,

TABLE 2. BAR MIGRATION DISTANCE/ ESTIMATED CHANNEL WIDTH

Width of bar method	Height of bar method
1.6	1.2–0.6
1.6	1.7–0.8
0.8	1.1–0.5
1.1	1.1–0.6
0.9	1.0–0.3
Average: 1.2	Average of median values: 0.89

TABLE 3. ESTIMATED DEPTH/WIDTH RATIOS

Depth	Width	Depth/width ratios
0.75	5.75	0.13
1.2	12.4	0.10
0.4	5.5	0.07
0.8	11.3	0.07
0.5	4.8	0.10
0.3	3.2	0.09

it is possible that the sinuosity could have been small enough that the rivers would have fallen into the "straight" category of Leopold and Wolman (1957), which was defined as channels with sinuosity less than 1.5. These channels are also classified today as "low sinuosity" channels or as "wandering" channels in other classification schemes (e.g., Church, 2006). However, straight channels are typified by downstream migrating alternate bars, and mid-channel bars in the case of wandering channels, in contrast to our observations. Because river dynamics are better classified according to the bar processes than the planform shape alone (Bridge, 2003), we contend that these were meandering channels with point bars and bend expansion but limited to lower sinuosity due to a relatively rapid rate of chute formation.

Using our estimated channel widths based on the width of bar method (Table 1) and our estimates of depth based on the thickness of lateral accretion surfaces with rollovers at the top, we estimated depth/width ratios for the Tapeats channels that range from 0.07 to 0.13 (Table 3). Lyster et al.'s (2022) compilation of ~1700 natural rivers indicates that depth/width ratios are capable of distinguishing single-thread from multi-thread rivers, with the former having ratios >0.02. Our estimates far exceed this value and thus support our interpretation that the Tapeats channels were single-thread, meandering rivers.

Channel Migration without Setup

The channel-form, lateral-accretion-set cross sections can be used for estimation of channel setup at times of abandonment, which allows for assessment of whether avulsions or chute cutoffs would have been more likely mechanisms of abandonment in each case. Several parts of the Tapeats beds suggest abandonment under very little or no bed accretion. Bed 1 records downlapping of foresets across most of the length of the base of the channel-form floor. The relatively flat upper surface and gently rising basal surface at the north end outline the channel margin. The switch from solely lateral migration to both lateral migration and vertical aggradation of the channel floor at the north end suggests that flow in the channel waned due to abandonment, and the remaining topographic depression was filled with sand and fine gravel to the approximate level of the floodplain, as designated by the elevation of the foreset rollover (Fig. 8). The final fill could have resulted from overbank flows, although the coarse grain sizes would be more consistent with delivery of sand through a tie channel.

Bed 2 also records downlapping of foresets across most of the length of the channel-form floor from the channel margin to the south to just prior to surface T_2 to the north. This includes pause plane 1 and its overlying shale layer that both draped and onlapped the point bar and channel floor (Figs. 9 and 7C). The shale (and the shale on pause plane 2) indicates a short-term episode of mud deposition within the channel, and suspension deposition of mud reflects an episode of sluggish flow during temporary abandonment, or partial abandonment, of the channel. The fact that strata deposited before and after pause plane 1 record solely lateral migration of the point bar without channel-floor deposition indicates no increase in setup. The examples in Beds 1 and 2 discussed above are interpreted to represent abandonment due to capture of flow by an incising channel, similar to chute cutoff.

Channel Setup

There are three examples of intervals in the Tapeats beds that record possible channel setups. One is the last phase of deposition in Bed 2, just prior to T_2 (Fig. 9). Using the position of the high point of rollover of the youngest downlapping lateral accretion surface as an approximate height of the floodplain at the time, and the immediate subsequent increase in the thalweg position due to channel-floor deposition, the setup would have been ~20 cm. Two other examples of possible channel setups are preserved in Bed 3, which is dominated by layers that record simultaneous lateral migration and channel-floor aggradation (Fig. 10), as opposed to lateral accretion surfaces that directly downlap the surfaces that defines the base of the channel complexes (most of Beds 1 and 2). This suggests that the depth of the channel may have remained relatively constant with an equivalent amount of aggradation in the channel floor and levee over time, i.e., channel setup.

We interpret the transitions between the three phases of deposition of Bed 3 (T_1 to T_2 and T_2 to T_3; Fig. 10) to reflect channel abandonment that could have resulted in part, or in full, from avulsion followed by reoccupation. Reoccupation led to erosional steepening of the channel margin at both transitions, particularly the T_1 to T_2 transition (Fig. 10). The reoccupation likely took place during a flood event, and since the marginal incision took place in coarse granular sediment (sand and gravel), this temporary widening of the channel may reflect adjustment during flooding to a critical shear stress of the bank material (Parker, 1978). Subsequent deposition of lateral accretion surfaces that directly downlap the newly sculpted channel floor indicate a phase of increased channel bend growth with little or no setup that was followed by another phase of increased setup with simultaneous point-bar migration and channel-floor aggradation. The final deposit of phase T_3 is recorded by a lenticular shale with a concave-up base that represents deposition of mud in ponded water in the very shallow remnant of the channel topography.

We measured the changes in stratigraphic position of the base of the channels, a measure of channel aggradation, for the three cases of possible setup described above (Table 4). Using the bar heights derived from rollovers as a proxy for channel depths, we calculated an avulsion setup percentage for each case (Table 4) using the following:

$$= (A_c/D)*100, \quad (1)$$

in which A_c is the channel aggradation and D is the channel depth. Avulsion typically occurs when channel aggradation is approximately equal to channel depth (Mohrig et al., 2000; Jerolmack and Mohrig, 2007). The threshold is commonly described in terms of a dimensionless avulsion time scale (Ta*; Ganti et al., 2014), calculated using measured time intervals between successive avulsions and both vertical aggradation rate and channel depth (Bryant et al., 1995; Jerolmack and Mohrig, 2007; Jerolmack, 2009; Reitz and Jerolmack, 2012; Ganti et al., 2014). Although Ta* is generally ~1 (= 100% avulsion setup; Ganti et al., 2014, their fig. 3d), rivers with small variance in discharge, such as the upstream reaches of the Huanghe River, can reach Ta* values of 10 (infrequent avulsions; Ganti et al., 2014).

The calculated T_2 Bed 2 avulsion setup is 25%, and the T_1–T_2 and T_2–T_3 setups are 56% and 75%, respectively (= Ta* of 0.56 and 0.75; Table 4), well less than ~100%, which is typical of modern (Ganti et al., 2014) and ancient (Mohrig et al., 2000) river systems. These are maximum values because some of the bar heights

TABLE 4. APPROXIMATE AVULSION SETUP ESTIMATES

		Increase in elevation of channel floor (m)	Original bar height (m)	Approximate avulsion setup (%)
Bed 2	Prior to T_2	0.2	0.8	25
Bed 3	T_1 to T_2	0.6	0.8	75
	T_2 to T_3	0.28	0.5	56

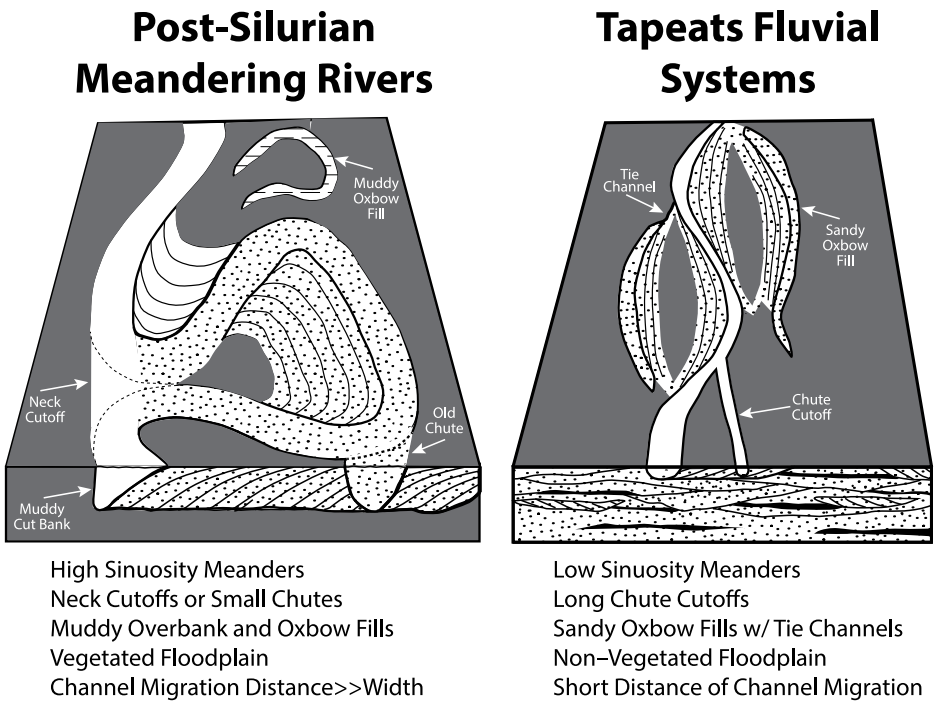

Figure 11. Comparison between post-Silurian meandering river systems that formed on vegetated land surfaces and our interpretation of lower sinuosity Tapeats Formation river systems that developed prior to land plants in the Cambrian.

are minimum values due to possible minor erosion at the top of the sets (i.e., incomplete rollover). These data indicate that the Tapeats rivers were abandoned when the channel setups were low—a maximum setup of three-fourths of the channel depth—thus suggesting either flow capture by incising chutes or avulsions of slightly to moderately perched channels due to breaching of relatively unstable cutbanks.

Stratal geometries provide insights into other morphodynamic behaviors, including the angle of climb of the channels as they increased their setups. The angles of climb of the three examples of possible setup, as measured directly from the photomosaics (Fig. 10), are very steep, ~5°–10°. Since meandering rivers typically migrate ~5–7 times the channel width or more before a neck cutoff (Howard and Knutson, 1984), if one assumes a width-to-depth ratio of 15 and a constant climb angle over time, a hypothetical channel setup of the Tapeats channels would have been 5.5–1 m, or equivalently 7.5–15 channel depths, over a complete cycle of meander bend growth to the point of neck cutoff. Thus, if the depths of the Tapeats channels were maintained during migration (not simply infilled), they would have increased their setups very quickly over short distances leading to avulsion or chute cutoff well before neck cutoff. These high rates of aggradation relative to lateral migration could have resulted from high sedimentation rates in flows that rapidly built up both the channel floor and levee systems, which would be consistent with flashy discharge, coarse sediment grain sizes, and proximity to small bedrock incised canyons (near the canyon–fan transition). Additionally, the high climb angle could have resulted from low lateral migration rates. This possibility would be inconsistent with the inferred low bank strengths due to minimal cohesive mud, but if the channels were relatively shallow and wide compared to modern counterparts, then fluid stresses acting on the banks might have been lower (boundary stress scales with flow depth). For a given sediment supply, lower bed and bank stresses could have reduced channel migration rates and increased bed accretion rates. Another possible factor is the average curvature of the channels, which creates centrifugal forces and secondary currents that drive greater sinuosity. The interpreted low sinuosity Tapeats channels might have reduced migration rates relative to aggradation rates, resulting in rapid climb. Regardless of the mechanism, the channels were unstable and prone to abandonment after short migration distances.

DISCUSSION

The results of our work allow us to reconstruct the ancient fluvial dynamics of the unvegetated Cambrian landscape of the Tapeats Formation. We present a facies model for these strata that should be applicable to pre-Silurian meandering river systems (Fig. 11). We agree with recent reconstructions of the Tapeats (Dehler et al., 2024), which indicate that the Payson, Arizona, region, including the Route 87S outcrop where the meandering river strata are exposed, was entirely fluvial and far from the ancient ocean to the west. The Route 87S outcrop is close to outcrops east of town with bedrock incised channel fills of cobble conglomerate, suggesting proximity to canyon–alluvial fan transitions. Such mountain-proximal locations with high slopes are areas where avulsion setups tend to be high due to spatial decelerations and deposition of sediment in channels (Parker et al., 1998, their fig. 3). However, the stratal geometries of the beds at the Route 87S site, and our paleohydraulic analysis, indicate that channel abandonment commonly took place early. Specifically, abandonment of channels took place after they had migrated only one to two channel widths, <~15% of the average meander loop distance of modern channels, which generally migrate across muddy floodplains to the point of neck cutoff. In addition, the stratal geometries indicate that much of the channel migration took place without significant channel setup, and abandonment events in such cases would have resulted from headward erosion of chute fronts during overbank flows, i.e., chute cutoffs. Frequent capture of much, or eventually all, of the channel flows by chutes acted to straighten the channels, terminating channel bend growth. Abandoned channels were primarily filled by coarse bedload material through tie channels, creating sandy, low-sinuosity, oxbow deposits (Fig. 11), although some fill could have been derived from overbank flows.

Our paleohydraulic analysis indicates that for the Tapeats beds that show evidence of setup, the degree of setup was well below the degree typical of avulsions (~100%) in modern meandering rivers, which suggests that if avulsions took place, they did so at early stages of meander growth at times of low sinuosity. As a result, abandonment took place when the bases of the channels sat below the level of the floodplain, which greatly increases the likelihood of future reoccupation of the channels, as evidenced by the phases of channel reorganization and deposition in Beds 2 and 3 (e.g., channel widening, shale drape deposition, transitions from solely point-bar deposition to point-bar and channel-floor deposition). Frequent reoccupation (up to 24%) was noted in studies of ancient strata (Mohrig et al., 2000). The fate of abandoned channels depends on the style and rate of infill. In modern meandering channels, the cutoff loop is often separated

from the main channel by a depositional wedge or plug at the junction forming an oxbow lake that eventually fills from tie-channel progradation and overbank sedimentation. We do not see evidence for lake infill, but it is possible that it would have a low preservation rate due to lateral migration and reworking. Alternatively, if the cutoff portion of the old channel and the new chute both remained active simultaneously, the planform morphology might have been one with multiple channels separated by islands of floodplain terrain (as in Fig. 11). Planform patterns of this type are often called anabranching or anastamosing on the modern Earth, and the stabilization of the islands by vegetation is thought to be a key ingredient to develop this pattern. We note that anastamosing is distinct from wandering or braiding because it contains multiple channels separated by non-channelized islands, whereas in wandering or braided rivers mid-channel bars separate flow pathways within a single channel (e.g., Church, 2006). We speculate that anastamosing patterns would be very rare or absent prior to vegetation because multi-channel systems would be less stable in the absence of land plants: lateral reworking of the islands would merge the channels into a single channel. The Tapeats deposits do not contain evidence for multiple channels being active simultaneously, and our estimates of depth/width ratios are consistent with single-thread rivers, and thus, we interpreted them as low sinuosity meandering channels.

The abandonment of channels with moderate to no setups by chute cutoffs and early avulsions indicates susceptibility of erosion of channel margins and flood plains. Low bank strength was likely related to the lack of vegetation and limited cohesive mud on the landscape. Vegetation acts to stabilize soils and resist erosion during overbank flooding (Tal and Paola, 2007; McMahon and Davies, 2018a; Gearon et al., 2024) and promotes mud deposition through flocculation (Zeichner et al., 2021). Specifically, resistance is derived from binding of sediment by roots, which increases shear stress thresholds for initiation of sediment transport. The vegetation also reduces flow velocity, increases drag, and leads to deposition of cohesive mud, all of which limits bed erosion (Tal and Paola, 2007; Davies and Gibling, 2010; Thorne, 1990; McMahon and Davies, 2018a, 2018b). The fact that the Tapeats deposits with meandering river facies (site 87S) contain <15% mudstone, and that the channel margins (e.g., Bed 2) and outer bank margins were cut primarily into sandstone and conglomerate, suggests that although there was mud on the floodplains at this time, they were primarily sandy. Previous work has emphasized the role of reduced bank strength (Burr et al., 2009; Lapôtre et al., 2019) for the development of sinuous single-thread rivers in areas without vegetation, which can be provided by cohesive mud in percentages as low as ~30% (Ganti et al., 2019). The mudstone percentages of the Tapeats are less than half of this value. The absence of vegetation likely yielded shallow cutbanks, low sinuosity, low setup values, less muddy floodplains, and thinner overbank mud deposits, all of which contrast strongly with most modern meandering river systems, which have thick, muddy floodplain deposits, steep to overhanging cut banks, large setups, and high sinuosity (Fig. 11).

The facies model that we present (Fig. 11) with low sinuosity rivers, easily erodible sandy channel banks and flood plains, and frequent abandonment events is supported by facies models for modern unvegetated meandering river systems. Such models emphasize (1) rapid lateral migration rates and reworking of unvegetated floodplains, (2) low topographic relief of levees, and (3) and greater hydraulic connectivity between channels and floodplains (Hasson et al., 2023), all of which leads to reworking of floodplains and coarser grained flood plain deposits (Ielpi et al., 2018). The Tapeats deposits suggest that the lack of vegetation and relatively sandy substrate made the floodplains relatively easy to erode, so that during floods, chutes may have quickly and easily developed between neighboring channel bends. An additional factor for early abandonment is high river discharge variability (flashy discharge), which Ganti et al. (2014) argue can lead to early avulsions at low setup values. Proximal settings, like the Tapeats fluvial system of the study area, tend to have higher setups that are generally greater than the channel depth (>100%), so flashy discharge may have been an additional factor in promoting early chute cutoffs during short-lived, overbank flooding events at low setup values during Tapeats deposition (Maitan et al., 2024).

In terms of the time scales of avulsions/cutoffs, these are not possible to accurately estimate for the Cambrian strata of the Tapeats Sandstone, but the lower Amargosa River (Death Valley, California, USA) is a modern example of a river with an unvegetated sinuous river channel with similar scale channels—<2 m deep (Douglas et al., 2025)—to those of the Tapeats that could be used as an analog, although it is a much muddier system. The Amargosa channels are up to 35 m wide, and they migrate laterally up to 200 m at rates of <1.5 m/yr (Ielpi, 2019). If one assumed a similar rate of channel migration for the Tapeats channels, they would preserve a record of several tens of years of migration, and many years to a few tens of years between episodes of partial avulsion and subsequent reoccupation and resetting of channel geometry and behavior.

CONCLUSIONS

The Cambrian Tapeats Formation of the Payson, Arizona, region records an east-to-west transition from cobble- and pebble-filled, bedrock-incised channels (a few meters deep) to sinuous, migrating channels that were primarily filled with poorly sorted sand and fine (granule to pebble) gravel. The close proximity (over ~10 km) of these facies regions suggests a proximal canyon–fan transition. A combination of lithofacies, paleocurrents, detailed mapping of cliff-face exposures, and paleohydraulic analysis allowed us to reconstruct fluvial dynamics of sinuous river systems of a pre-Silurian, unvegetated landscape. Outcrops in the town of Payson consist of stacked, meter-scale, channel-fill deposits of granule to pebble conglomerate, pebbly sandstone, and medium-grained sandstone with point-bar lateral accretion surfaces. Stratal geometries indicate low-angle outer-bend channel margins (~10°), which reflect a paucity of floodplain mud and relatively erodible granular cutbanks. Episodes of channel abandonment took place after channels had migrated only 1–2 channel widths. In some cases, there was little or no channel-bed aggradation prior to abandonment, suggesting a chute cutoff mechanism. In other cases, abandonment took place after the channel setup (superelevation of bankfull water level above the floodplain) was only 25%–75% of the bankfull depth, indicating possible avulsion, but at setup values below those of modern rivers with muddy banks (~100%).

Our results highlight the differences between sinuous channels with unstable banks in unvegetated landscapes with frequent chute cutoffs and avulsions, and most modern meandering rivers that traverse muddy floodplains in which the channel bends commonly grow to the point of neck cutoff. Our facies model also differs from those developed for braided rivers, which are commonly applied to pre-Silurian fluvial lithofacies, and it highlights the geomorphological and paleohydraulic aspects of sinuous channels that were frequently abandoned as they migrated across unvegetated, relatively mud-poor floodplains. The model can be applied to the deposits of past and present single-threaded rivers of unvegetated landscapes on Earth and other planetary bodies.

ACKNOWLEDGMENTS

P.M. Myrow acknowledges Colorado College for support. R.R. Gaines was supported by a Hirsch Research Initiation Grant from Pomona College, as well as by the Pomona College Academic Dean's Office. M.P. Lamb acknowledges Caltech for support.

REFERENCES CITED

Bridge, J.S., 2003, Rivers and Floodplains: Forms, Processes, and Sedimentary Record: John Wiley & Sons, 491 p.

Bryant, M., Falk, P., and Paola, C., 1995, Experimental study of avulsion frequency and rate of deposition: Geology, v. 23, p. 365–368, https://doi.org/10.1130/0091-7613(1995)023<0365:ESOAFA>2.3.CO;2.

Burr, D.M., Enga, M.T., Williams, R.M., Zimbelman, J.R., Howard, A.D., and Brennand, T.A., 2009, Pervasive aqueous paleoflow features in the Aeolis/Zephyria Plana region, Mars: Icarus, v. 200, p. 52–76, https://doi.org/10.1016/j.icarus.2008.10.014.

Church, M., 2006, Bed material transport and the morphology of alluvial river channels: Annual Review of Earth and Planetary Sciences, v. 34, p. 325–354, https://doi.org/10.1146/annurev.earth.33.092203.122721.

Colwyn, D.A., Sheldon, N.D., Maynard, J.B., Gaines, R., Hofmann, A., Wang, X., Gueguen, B., Asael, D., Reinhard, C.T., and Planavsky, N.J., 2019, A paleosol record of the evolution of Cr redox cycling and evidence for an increase in atmospheric oxygen during the Neoproterozoic: Geobiology, v. 17, p. 579–593, https://doi.org/10.1111/gbi.12360.

Cotter, E., 1978, The evolution of fluvial style, with special reference to the central Appalachian Paleozoic, *in* Miall, A.D., ed., Fluvial Sedimentology: Canadian Society of Petroleum Geologists Memoir 5, p. 361–382.

Davies, N.S., and Gibling, M.R., 2010, Paleozoic vegetation and the Siluro-Devonian rise of fluvial lateral accretion sets: Geology, v. 38, p. 51–54, https://doi.org/10.1130/G30443.1.

Dehler, C., Sundberg, F., Karlstrom, K., Crossey, L., Schmitz, M., Rowland, S., and Hagadorn, J., 2024, The Cambrian of the Grand Canyon: Refinement of a classic stratigraphic model: GSA Today, v. 34, no. 11, p. 4–11, https://doi.org/10.1130/GSATG604A.1.

DiBiase, R.A., Limaye, A.B., Scheingross, J.S., Fischer, W.W., and Lamb, M.P., 2013, Deltaic deposits at Aeolis Dorsa: Sedimentary evidence for a standing body of water on the northern plains of Mars: Journal of Geophysical Research: Planets, v. 118, p. 1285–1302, https://doi.org/10.1002/jgre.20100.

Douglas, M.M., Miller, K.L., and Lamb, M.P., 2025, Mud cohesion governs unvegetated meander migration rates and deposit architecture: Geological Society of America Bulletin, v. 137, p. 522–540, https://doi.org/10.1130/B37315.1.

Elston, D.P., and Bressler, S.L., 1977, Paleomagnetic poles and polarity zonation from Cambrian and Devonian strata of Arizona: Earth and Planetary Science Letters, v. 36, p. 423–433, https://doi.org/10.1016/0012-821X(77)90067-X.

Fedo, C.M., and Cooper, J.D., 1990, Braided fluvial to marine transition; the basal Lower Cambrian Wood Canyon Formation, southern Marble Mountains, Mojave Desert, California: Journal of Sedimentary Research, v. 60, p. 220–234.

Galeazzi, C.P., Almeida, R.P., and do Prado, A.H., 2021, Linking rivers to the rock record: Channel patterns and paleocurrent circular variance: Geology, v. 49, p. 1402–1407, https://doi.org/10.1130/G49121.1.

Ganti, V., Chu, Z., Lamb, M.P., Nittrouer, J.A., and Parker, G., 2014, Testing morphodynamic controls on the location and frequency of river avulsions on fans versus deltas: Huanghe (Yellow River), China: Geophysical Research Letters, v. 41, p. 7882–7890, https://doi.org/10.1002/2014GL061918.

Ganti, V., Whittaker, A.C., Lamb, M.P., and Fischer, W.W., 2019, Low gradient, single-threaded rivers prior to greening of the continents: Proceedings of the National Academy of Science, v. 116, p. 11,652–11,657, https://doi.org/10.1073/pnas.1901642116.

Gearon, J.H., Martin, H.K., DeLisle, C., Barefoot, E.A., Mohrig, D., Paola, C., and Edmonds, D.A., 2024, Rules of river avulsion change downstream: Nature, v. 634, p. 91–95, https://doi.org/10.1038/s41586-024-07964-2.

Greenberg, E., Ganti, V., and Hajek, E., 2021, Quantifying bankfull flow width using preserved bar clinoforms from fluvial strata: Geology, v. 49, p. 1038–1043, https://doi.org/10.1130/G48729.1.

Hasson, M., Marvin, M.C., Gunn, A., Ielpi, A., and Lapôtre, M.G., 2023, A depositional model for meandering rivers without land plants: Sedimentology, v. 70, p. 2272–2301, https://doi.org/10.1111/sed.13121.

Hayden, A.T., Lamb, M.P., and Carney, A.J., 2021, Similar curvature-to-width ratios for channels and channel belts: Implications for paleo-hydraulics of fluvial ridges on Mars: Geology, v. 49, p. 837–841, https://doi.org/10.1130/G48370.1.

Hereford, R., 1977, Deposition of the Tapeats sandstone (Cambrian) in central Arizona: Geological Society of America Bulletin, v. 88, p. 199–211, https://doi.org/10.1130/0016-7606(1977)88<199:DOTTSC>2.0.CO;2.

Hooke, J., 2023, Morphodynamics of active meandering rivers reviewed in a hierarchy of spatial and temporal scales: Geomorphology, v. 439, https://doi.org/10.1016/j.geomorph.2023.108825.

Howard, A.D., and Knutson, T.R., 1984, Sufficient conditions for river meandering: A simulation approach: Water Resources Research, v. 20, p. 1659–1667, https://doi.org/10.1029/WR020i011p01659.

Ielpi, A., 2017, Lateral accretion of modern unvegetated rivers: Remotely sensed fluvial–aeolian morphodynamics and perspectives on the Precambrian rock record: Geological Magazine, v. 154, p. 609–624, https://doi.org/10.1017/S001675681600025X.

Ielpi, A., 2019, Morphodynamics of meandering streams devoid of plant life: Amargosa River, Death Valley, California: Geological Society of America Bulletin, v. 131, p. 782–802, https://doi.org/10.1130/B31960.1.

Ielpi, A., and Ghinassi, M., 2015, Planview style and palaeodrainage of Torridonian channel belts: Applecross formation, Stoer Peninsula, Scotland: Sedimentary Geology, v. 325, p. 1–16, https://doi.org/10.1016/j.sedgeo.2015.05.002.

Ielpi, A., and Rainbird, R.H., 2016, Reappraisal of Precambrian sheet-braided rivers: Evidence for 1.9 Ga deep-channelled drainage: Sedimentology, v. 63, p. 1550–1581, https://doi.org/10.1111/sed.12273.

Ielpi, A., Rainbird, R.H., Ventra, D., and Ghinassi, M., 2017, Morphometric convergence between Proterozoic and post-vegetation rivers: Nature Communications, v. 8, https://doi.org/10.1038/ncomms15250.

Ielpi, A., Ghinassi, M., Rainbird, R.H., and Ventra, D., 2018, Planform sinuosity of Proterozoic rivers: A craton to channel-reach perspective, *in* Ghinassi, M., Colombera, L., Mountney, N.P., Reesink, A.J.H., and Bateman, B., eds., Fluvial Meanders and Their Sedimentary Products in the Rock Record: International Association of Sedimentary Geologists Special Publication, v. 48, p. 81–118, https://doi.org/10.1002/9781119424437.ch4.

Jerolmack, D.J., 2009, Conceptual framework for assessing the response of delta channel networks to Holocene sea level rise: Quaternary Science Reviews, v. 28, p. 1786–1800, https://doi.org/10.1016/j.quascirev.2009.02.015.

Jerolmack, D.J., and Mohrig, D., 2007, Conditions for branching in depositional rivers: Geology, v. 35, p. 463–466, https://doi.org/10.1130/G23308A.1.

Karlstrom, K.E., Mohr, M.T., Schmitz, M.D., Sundberg, F.A., Rowland, S.M., Blakey, R., Foster, J.R., Crossey, L.J., Dehler, C.M., and Hagadorn, J.W., 2020, Redefining the Tonto Group of Grand Canyon and recalibrating the Cambrian time scale: Geology, v. 48, p. 425–430, https://doi.org/10.1130/G46755.1.

Karlstrom, K., Hagadorn, J., Gehrels, G., Matthews, W., Schmitz, M., Madronich, L., Mulder, J., Pecha, M., Giesler, D., and Crossey, L., 2018, Cambrian Sauk transgression in the Grand Canyon region redefined by detrital zircons: Nature Geoscience, v. 11, p. 438–443, https://doi.org/10.1038/s41561-018-0131-7.

Kite, E.S., Howard, A.D., Lucas, A., and Lewis, K.W., 2015, Resolving the era of river-forming climates on Mars using stratigraphic logs of river-deposit dimensions: Earth and Planetary Science Letters, v. 420, p. 55–65, https://doi.org/10.1016/j.epsl.2015.03.019.

Lapôtre, M.G.A., Ielpi, A., Lamb, M.P., Williams, R.M.E., and Knoll, A.H., 2019, Model for the formation of single-thread rivers in barren landscapes and implications for pre-Silurian and Martian fluvial deposits: Journal of Geophysical Research: Earth Surface, v. 124, p. 2757–2777, https://doi.org/10.1029/2019JF005156.

Leopold, L.B., and Wolman, M.G., 1957, River channel patterns: Braided, meandering, and straight: U.S. Geological Survey Professional Paper 282-B, 50 p., https://doi.org/10.3133/pp282B.

Long, D.G.F., 1978, Proterozoic stream deposits: Some problems of recognition and interpretation of ancient sandy fluvial systems, *in* Miall, A.D, ed., Fluvial Sedimentology: Calgary, Alberta, Canada, Canadian Society of Petroleum Geology, v. 5, p. 313–342.

Long, D.G.F., 2011, Architecture and depositional style of fluvial systems before land plants: A comparison of Precambrian, early Paleozoic and modern river deposits, *in* Davidson, S., Leleu, S., and North, C.P., eds., From River to Rock Record: The Preservation of Fluvial Sediments and Their Subsequent Interpretation: SEPM (Society for Sedimentary Geology) Special Publication, v. 97, p. 37–61, https://doi.org/10.2110/sepmsp.097.037.

Lyster, S.J., Whittaker, A.C., and Hajek, E.A., 2022, The problem of paleo-planforms: Geology, v. 50, p. 822–826, https://doi.org/10.1130/G49867.1.

Maitan, R., Finotello, A., Tognin, D., D'Alpaos, A., Fielding, C.R., Ielpi, A., and Ghinassi, M., 2024, Hydrologically driven modulation of cutoff regime in meandering rivers: Geology, v. 52, p. 336–340, https://doi.org/10.1130/G51783.1.

Matthews, W., Guest, B., and Madronich, L., 2018, Latest Neoproterozoic to Cambrian detrital zircon facies of western Laurentia: Geosphere, v. 14, p. 243–264, https://doi.org/10.1130/GES01544.1.

Matsubara, Y., Howard, A.D., Burr, D.M., Williams, R.M., Dietrich, W.E., and Moore, J.M., 2015, River meandering on Earth and Mars: A comparative study of Aeolis Dorsa meanders, Mars and possible terrestrial analogs of the Usuktuk River, AK, and the Quinn River, NV: Geomorphology, v. 240, p. 102–120, https://doi.org/10.1016/j.geomorph.2014.08.031.

McMahon, W.J., and Davies, N.S., 2018a, Evolution of alluvial mudrock forced by early land plants: Science, v. 359, p. 1022–1024, https://doi.org/10.1126/science.aan4660.

McMahon, W.J., and Davies, N.S., 2018b, The shortage of geological evidence for pre-vegetation meandering rivers, *in* Ghinassi, M., Colombera, L., Mountney, N.P., Reesink, A.J.H., and Bateman, B., eds., Fluvial Meanders and Their Sedimentary Products in the Rock Record: International Association of Sedimentary Geologists Special Publication, v. 48, p. 119–148, https://doi.org/10.1002/9781119424437.ch5.

Mohrig, D., Heller, P.L., Paola, C., and Lyons, W.L., 2000, Interpreting avulsion process from ancient alluvial sequences: Guadalope–Matarranya system (northern Spain) and Wasatch Formation (western Colorado): Geological Society of America Bulletin, v. 112, p. 1787–1803, https://doi.org/10.1130/0016-7606(2000)112<1787:IAPFAA>2.0.CO;2.

Parker, G., 1978, Self-formed straight rivers with equilibrium banks and mobile bed. Part 2. The gravel river: Journal of Fluid Mechanics, v. 89, p. 127–146, https://doi.org/10.1017/S0022112078002505.

Parker, G., Paola, C., Whipple, K.X., and Mohrig, D., 1998, Alluvial fans formed by channelized fluvial and sheet flow. I: Theory: Journal of Hydraulic Engineering, v. 124, p. 985–995, https://doi.org/10.1061/(ASCE)0733-9429(1998)124:10(985).

Parker, G., Wilcock, P.R., Paola, C., Dietrich, W.E., and Pitlick, J., 2007, Physical basis for quasi-universal relations describing bankfull hydraulic geometry of single-thread gravel bed rivers: Journal of Geophysical Research: Earth Surface, v. 112, F4, F04005, https://doi.org/10.1029/2006JF000549.

Reitz, M.D., and Jerolmack, D.J., 2012, Experimental alluvial fan evolution: Channel dynamics, slope controls, and shoreline growth: Journal of Geophysical Research: Earth Surface, v. 117, F2, F02021, https://doi.org/10.1029/2011JF002261.

Rose, E.C., 2006, Nonmarine aspects of the Cambrian Tonto Group of the Grand Canyon, USA, and broader implications: Palaeoworld, v. 15, p. 223–241, https://doi.org/10.1016/j.palwor.2006.10.008.

Santos, M.G.M., and Owen, G., 2016, Heterolithic meandering-channel deposits from the Neoproterozoic of NW Scotland: Implications for palaeogeographic reconstructions of Precambrian sedimentary environ-

ments: Precambrian Research, v. 272, p. 226–243, https://doi.org/10.1016/j.precamres.2015.11.003.

Sarkar, S., Samanta, P., Mukhopadhyay, S., and Bose, P.K., 2012, Stratigraphic architecture of the Sonia Sandstone interval, India in its Precambrian context: Precambrian Research, v. 214–215, p. 210–226, https://doi.org/10.1016/j.precamres.2012.01.001.

Tal, M., and Paola, C., 2007, Dynamic single-thread channels maintained by the interaction of flow and vegetation: Geology, v. 35, p. 347–350, https://doi.org/10.1130/G23260A.1.

Thorne, C.R., 1990, Effects of vegetation on riverbank erosion and stability, *in* Thornes, J.B., ed., Vegetation and Erosion: Processes and Environments: Chichester, West Sussex, England, John Wiley, p. 125–144.

Valenza, J., Ganti, V., Whittaker, A.C., and Lamb, M.P., 2023, Pre-vegetation, single-threaded rivers sustained by cohesive, fine-grained bank sediments: Mesoproterozoic Stoer Group, NW Scotland: Geophysical Research Letters, v. 50, https://doi.org/10.1029/2023GL104379.

Went, D.J., 2017, Alluvial fan, braided river and shallow marine turbidity current deposits in the Port Lazo and Roche Jagu formations, Northern Brittany: Relationships to andesite emplacements and implications for age of the Plourivo–Plouézec Group: Geological Magazine, v. 154, p. 1037–1060, https://doi.org/10.1017/S0016756816000686.

Zeichner, S.S., Nghiem, J., Lamb, M.P., Takashima, N., de Leeuw, J., Ganti, V., and Fischer, W.W., 2021, Early plant organics increased global terrestrial mud deposition through enhanced flocculation: Science, v. 371, p. 526–529, https://doi.org/10.1126/science.abd0379.

Science Editor: Mihai Ducea
Associate Editor: Ganqing Jiang

Manuscript Received 15 February 2025
Revised Manuscript Received 16 June 2025
Manuscript Accepted 1 August 2025